Magnetic properties of ferrihydrite nanoparticles doped with Ni, Mo, and Ir

A. Punnoose and T. Phanthavady
Department of Physics, Boise State University, Boise, Idaho 83725, USA

M. S. Seehra*
Department of Physics, West Virginia University, Morgantown, West Virginia 26506-6315, USA

N. Shah and G. P. Huffman
The Consortium for Fossil Fuel Science, University of Kentucky, Lexington, Kentucky 40506, USA
(Received 8 April 2003; revised manuscript received 16 September 2003; published 26 February 2004)

In this work, changes in the magnetic properties of ferrihydrite (FHYD) nanoparticles (formula $FeOOH \cdot nH_2O$; size$\simeq$5 nm) on doping with 5 at.% each of Ni, Mo, and Ir by coprecipitation are reported. The variations of magnetization M as a function of magnetic field H (up to $\pm$50 kOe) and temperature T (5–375 K) were investigated for the four samples, viz., FHYD, Ni/FHYD, Mo/FHYD, and Ir/FHYD, both for the zero-field-cooled (ZFC) and field-cooled (FC) conditions. The T variation of the low-field ($H=100$ Oe) magnetic susceptibility χ (ZFC) peaks at temperature $T_p \simeq 70$, 47, 43, and 34 K for FHYD, Ni/FHYD, Mo/FHYD, and Ir/FHYD, respectively. For $T<T_p$, χ (ZFC)$<\chi$ (FC), and χ (FC) shows broad minima at $T_s=30$, 27, 22, and 16 K for FHYD, Ni/FHYD, Mo/FHYD, and Ir/FHYD, respectively. The data are analyzed in terms of the modified Langevin function $M=M_0\mathcal{L}(\mu_p H/kT)+\chi_a H$, where μ_p is the magnetic moment/particle and k is the Boltzmann constant. From the analysis of the data, temperature-independent $\mu_p=369$, 375, 237, and $239\mu_B$ are determined for FHYD, Ni/FHYD, Mo/FHYD, and Ir/FHYD, respectively. It is argued that the decrease in T_p and T_s noted above with doping results from shape anisotropy due to demagnetization fields. For $T \leqslant T_s$, the presence of exchange anisotropy may indicate spin-glass-like ordering of the surface spins. In this temperature regime, a steplike magnetization reversal behavior is observed in the low-field region of the hysteresis loops, in qualitative agreement with the theoretical predictions by Fraerman *et al.* [Phys. Rev. B **65**, 184433 (2002)] for magnetic nanoparticles with interparticle interaction. Finally, from the observed magnitude of μ_p, it is inferred that Ni substitutes for Fe throughout the nanoparticle, whereas doping with Mo and Ir occurs primarily at the surface.

DOI: 10.1103/PhysRevB.69.054425 PACS number(s): 75.50.Tt, 75.50.Ee, 75.75.+a, 75.20.−g

I. INTRODUCTION

Ferrihydrite with the general formula $FeOOH \cdot nH_2O$ is a widespread iron oxyhydroxide which occurs naturally in the 3–5 nm particle size range and is also easily synthesized.[1,2] Ferrihydrite (FHYD) is a precursor to other iron oxides[3] and is related to ferritin, the iron reservoir in living organisms, containing FHYD core encapsulated in a protein shell.[4] Because of their small size, FHYD nanoparticles (NP) have also been used as catalysts and absorbents.[1,5]

Magnetism of NP systems is of interest because of their technological applications and because their magnetic properties differ substantially from their bulk counterparts due to the increasing role of the surface spins as the particle size is decreased.[6] The antiferromagnetic (AF) NP systems below their Néel temperature T_N provide a particularly interesting case since any observed magnetic moment must result from uncompensated spins. Also, not all AF-NP systems are alike since the observed moment depends on the nature of AF ordering as first suggested by Néel[7] and elaborated by Richardson *et al.*[8] These differences have been reported in recent studies of NP systems of NiO (Ref. 9) and CuO (Ref. 10) *vis-à-vis* ferritin and FHYD.[11] In general, the surface spins have reduced coordination and broken exchange bonds which can even affect the nature of ordering in the spins of the core of NP because of the exchange coupling between the surface and the core spins.[6] A recent study from our group using neutron diffraction and magnetometry on the deuterated FHYD (Ref. 12) showed that $T_N \simeq 350$ K, with a peak in dc magnetic susceptibility χ occurring at $T_p \simeq 65$ K. For $T<T_p$, the field-cooled (FC) and the zero-field-cooled (ZFC) χ bifurcate, indicative of blocking or a spin-glass transition at T_p. A magnetic moment/particle $\mu_p \simeq 300\mu_B$ observed in FHYD could be explained by a random distribution of uncompensated spins of Fe^{3+}.[12]

A way to investigate the unique features of AF-NP systems is by monitoring the changes in the magnetic properties produced by intentional doping by magnetic and nonmagnetic ions. In this work, we follow this approach by carrying out detailed magnetic studies in FHYD-NP doped with 5% each of Ni, Mo, and Ir. These dopants are of interest in part because of the resulting improvement in the catalytic properties of FHYD.[13] It is generally believed that the structure of FHYD is associated with that of the hematite (α-Fe_2O_3) except that the poor crystallinity of FHYD is explained on the basis of replacing some oxygens by OH and/or H_2O and by vacant Fe sites.[1] On the basis of XAFS (x-ray-absorption fine-structure) spectroscopy, it has been inferred that the Fe in the core of FHYD is octahedrally coordinated by three O and three OH groups, whereas the surface Fe atoms are tetrahedrally coordinated by O, OH, and H_2O.[1,5] Since there are coordinated unsaturated sites on the surface, it is likely

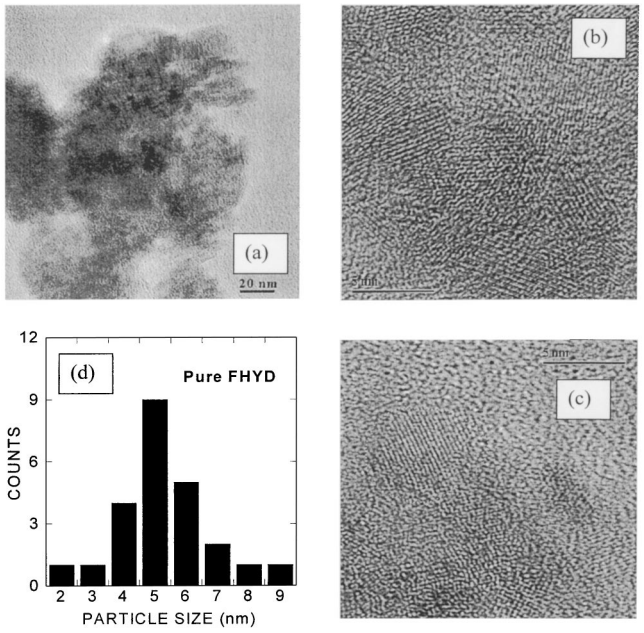

FIG. 1. High-resolution transmission electron microscopy images (a)–(c) and particle size distribution (d) of undoped FHYD. Circle in (c) shows a separate particle as evident from the atomic planes. Micron bars shown in (a), (b), and (c) represent 20, 5, and 5 nm, respectively.

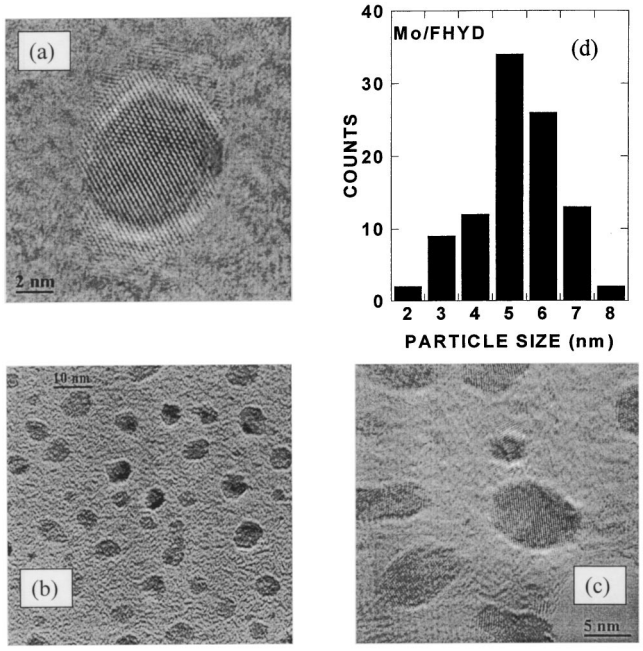

FIG. 2. High-resolution transmission electron microscopy images (a)–(c) and particle size distribution (d) of Mo/FHYD. Micron bars shown in (a), (b), and (c) represent 2, 10, and 5 nm, respectively.

that the dopants preferably occupy the surface sites, which should in turn affect μ_p, the magnetic moment/particle. In preliminary studies on Si-doped FHYD, a decrease in μ_p with an increase in Si content has been reported.[14] In the studies reported here, we have carried out a detailed analysis of the temperature (T) and magnetic field (H) variation of the magnetization in FHYD-NP doped with Ni, Mo, and Ir (5%), and these results are compared with those of the undoped FHYD-NP.

II. EXPERIMENTAL DETAILS

The FHYD samples were prepared by the coprecipitation method, the details of which have been given elsewhere.[1,2,5] For Ni/FHYD, appropriate amounts of nitrates of Fe and Ni are reacted with ammonium hydroxide to bring the pH to 10. For Mo/FHYD, ammonium hydroxide was added to a solution of $Fe(NO_3)_3 \cdot 9H_2O$ and $(NH_4)_6 \cdot Mo_7O_{24} \cdot 4H_2O$ mixed in appropriate amounts to bring the pH to 10. For preparing Ir/FHYD, $IrCl_3 \cdot 3H_2O$ was used similarly along with iron nitrate and ammonium hydroxide. The precipitates formed in each case were filtered, oven-dried in air at 50 °C, and then ground to a fine powder. The 5% concentration represents the atomic ratio $M/(M+\mathrm{Fe})$, where $M=$ Ni, Mo, or Ir.

The samples were characterized by x-ray diffraction (XRD) using Cu $K\alpha$ radiation ($\lambda = 1.541\,85$ Å) in a Rigaku diffractometer. The room-temperature XRD patterns for all four samples yielded the well-known two-line structure of FHYD,[1,12] although there are subtle differences between the four cases. For example, for Ni/FHYD, the two broad lines are sharper, and some weak lines, characteristic of six-line FHYD,[1] begin to become noticeable. The samples were also characterized by TEM (transmission electron microscopy) after appropriately diluting the samples in alcohol. In all four samples, observing the individual nanoparticles was difficult due to excessive agglomeration. However, for the undoped ferrihydrite and Mo-doped ferrihydrite, detailed analysis could be carried out on the size, shape, and particle distribution as illustrated in Figs. 1 and 2, respectively. The histograms were plotted by measuring the particle size of a large number of particles from the TEM images. In the case of highly agglomerated pure FHYD samples, the particle dimensions were identified based on the pattern of the atomic planes. The size distributions are centered around 5 nm for FHYD and 5.5 nm for Mo/FHYD. For Ni/FHYD and Ir/FHYD, excessive agglomeration prevented determination of the particle size.

Measurements of magnetization M as a function of H and T were made with a commercial superconducting quantum interference device (SQUID) magnetometer. Measurements were carried out on tightly packed powder samples placed in a white plastic drinking straw. The data reported here were corrected for the background signal from the sample holder with $\chi = M/H = -2.3 \times 10^{-8}$ emu/Oe, independent of H and T.[12]

III. EXPERIMENTAL RESULTS AND ANALYSIS

A. Temperature variation of the low-field magnetic susceptibility

The χ versus T data measured in the zero-field-cooled (ZFC) condition for all the samples peaks at a certain temperature T_p (Fig. 3).[15] For $T > T_p$, data from the field-cooled

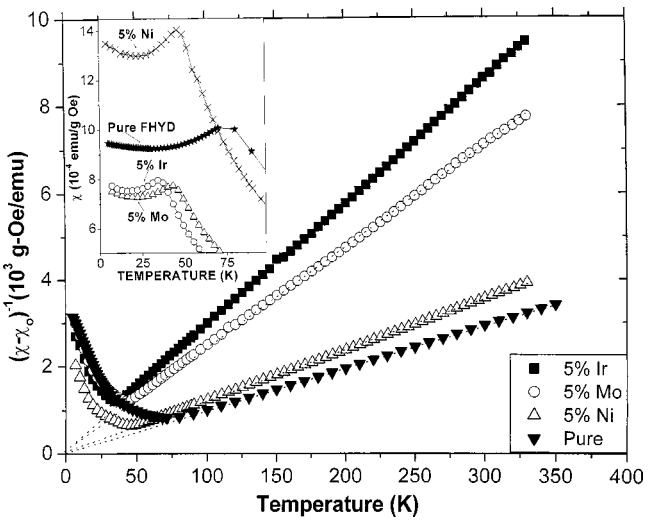

FIG. 3. Plots of $(\chi-\chi_0)^{-1}$ vs T, obtained using the temperature dependence of magnetic susceptibility χ measured with $H=100$ Oe for the ZFC samples [χ_0 is defined in Eq. (3)]. The dotted lines are extrapolations from the high-temperature linear parts. The inset shows the temperature dependence of χ measured under FC conditions for the four samples.

(FC) and ZFC measurements are identical, whereas for $T<T_p$, χ (FC)$>\chi$ (ZFC), similar to the observations reported in other AF-NP systems such as NiO,[9] ferritin,[4] and deuterated FHYD.[12] Note that χ (FC) below T_p goes through a minimum at a temperature T_s (Fig. 3). The magnitudes of T_p, T_s, and other relevant parameters are listed in Table I.

For ferritin[4] and deuterated FHYD,[12] the variations of M against H and T for $T_p<T<T_N$ were fitted to the modified Langevin function

$$M=M_0\mathcal{L}(\mu_pH/kT)+\chi_aH. \tag{1}$$

Here M_0 is the saturation magnetization, μ_p is the average magnetic moment per particle, χ_a is the AF susceptibility, k is the Boltzmann constant, and $\mathcal{L}(x)=\coth(x)-(1/x)$ is the Langevin function. The fits of the data to Eq. (1) at different T yielded M_0, which varied approximately linearly with T as[4,12]

$$M_0=M^*[1-(T/T_N)]. \tag{2}$$

Recently, Seehra and Punnoose[11] have shown that in the limit $\mu_pH/k_BT\ll 1$, Eq. (1) and Eq. (2) lead to $\chi=M/H$ given by

$$\chi=\chi_0+(C/T), \tag{3}$$

where $C=\mu_pM^*/3k$ and $\chi_0=\chi_a-(C/T_N)$. Equation (3) was found to fit the experimental χ versus T for both FHYD and ferritin above T_p.[11] A similar analysis is used for the low-field M versus T data obtained for these pure and doped FHYD samples also using the above relation [Eq. (3)], and the expected superparamagnetic behavior was observed. Weak deviations from linearity were observed in the plots of χ^{-1} versus T for $T>T_p$, similar to our recently reported studies in pure FHYD and ferritin.[11] The plots of $(\chi-\chi_0)^{-1}$ versus T, shown in Fig. 3, gave the expected linear variation, and the extrapolated lines go essentially through the origin using data for $T>T_p$.

B. Magnetic-field variation of magnetization

In Fig. 4, we show the experimental M versus H data for the four samples at various temperatures above T_p. In the earlier reported studies on FHYD,[12] χ_a was determined from the linear component of the M versus H variations at high H. However, it is obvious that χ_a so determined very likely contains some contribution from $\mathcal{L}(x)$ since $\mathcal{L}(x)$ is not saturated, particularly at higher temperatures. In this work, we estimated the values of χ_a, μ_p, and M_0 at different temperatures for the four samples simultaneously by fitting the data of Fig. 4 directly to Eq. (1) using a MATHCAD computer fitting program. The solid lines in Fig. 4 are the Langevin fits using Eq. (1). The magnitudes of χ_a obtained are listed in Table I. In Fig. 5, we have plotted χ_a determined from the Langevin analysis, which shows a temperature dependence. In Fig. 6, the plots of $(M-\chi_aH)/M_0$ against H/T are shown for the four samples, where lines through the points are fits to the Langevin function [Eq. (1)], using μ_p as the fitting parameter. The data for different T collapse very well into a single curve for all the four samples indicating a temperature-independent μ_p. As observed for ferritin[4] and FHYD,[12] M_0 is temperature-dependent. In Fig. 7, we show plots of M_0 against T for the four samples. The variations are clearly linear in the temperature range investigated. Extrapolating this linear variation to $M_0=0$ yields T_N. The temperature-independent values of μ_p estimated from the Langevin analysis as a function of temperature for the four samples are shown in Fig. 8, whereas the magnitudes obtained are listed in Table I. The estimates of T_N obtained by the linear extrapolation of the M_0 versus T plots to the limit $M_0=0$ are also listed in Table I. The value of $T_N=478$ K

TABLE I. Summary of the magnetic parameters obtained from different measurements and analyses for FHYD, Ni/FHYD, Mo/FHYD, and Ir/FHYD.

Material	T_P (K) (±1)	T_S (K) (±1)	T_N (K) (extrapolated) (±8)	χ_0 (10^{-5} emu/g Oe) (±0.8)	χ_a from the Langevin fit (10^{-5} emu/g Oe)	μ_p (in μ_B) from the Langevin fit (±10)
Pure FHYD	70	30	478	−15.9	7.4–10.8	369
Ni/FHYD	47	27	462	−13.0	8.9–13.3	375
MO/FHYD	43	22	423	−5.6	7.1–11.5	237
Ir/FHYD	34	16	420	−4.6	6.1–10.5	239

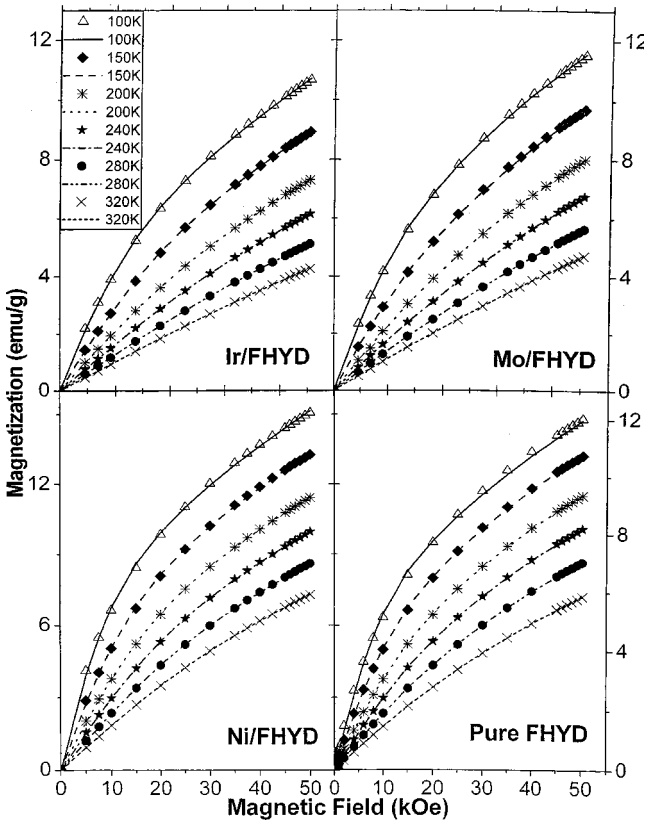

FIG. 4. Measured magnetizations of the four samples as a function of the applied magnetic field at fixed temperatures shown. The lines are theoretical fits using Eq. (1).

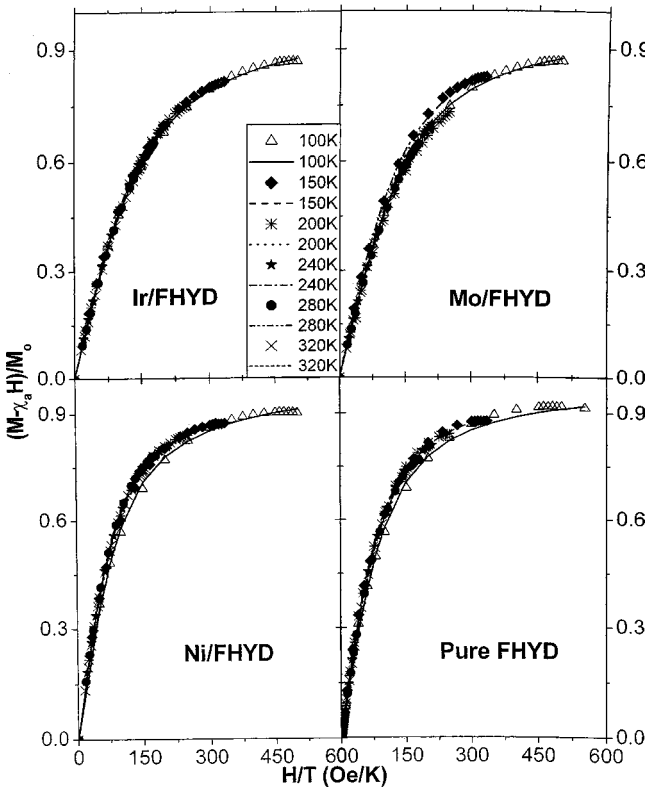

FIG. 6. Plots of Langevin function $\mathcal{L}(x)=(M-\chi_a H)/M_0$ from Eq. (1) against H/T for the four samples. The lines are calculated $\mathcal{L}(\mu_p H/k_B T)$ using μ_p as the fitting parameter (see Fig. 8).

obtained for pure FHYD from this analysis is significantly higher than the $T_N=350$ K determined from a recent neutron-scattering study.[12] A similar difference in the magnitudes of T_N was reported for ferritin based on a similar analysis by Makhlouf *et al.*[4] also. In that case, a T_N of 460 K was estimated from the M_0 versus T plot as compared to $T_N=240$ K reported from other studies. Although the experimental M_0 versus T data appear to be linear in the limited range investigated, the linear extrapolation method to determine the T_N seems questionable. It is noted that the temperature variation of the order parameter from neutron-diffraction studies of pure FHYD did not show a true linear variation.[12] Therefore, combined investigations of neutron diffraction and magnetometry on these samples may be required to understand this problem.

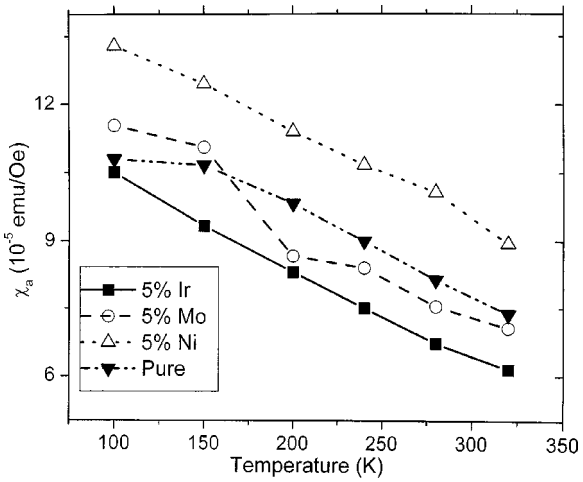

FIG. 5. Plots showing the temperature dependence of χ_a of Eq. (1) determined from the M vs H data of Fig. 4, using the Langevin function. The lines connecting the points are drawn for clarity.

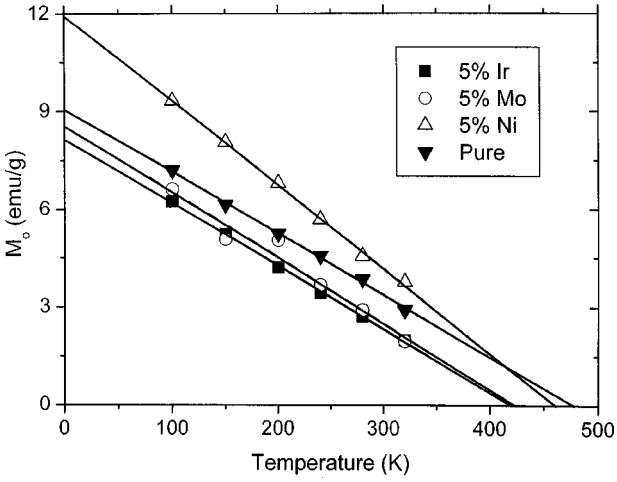

FIG. 7. Plots of M_0 vs T for the four samples. The lines are linear fits showing extrapolations for determining M^* for $T=0$ and T_N for $M_0=0$.

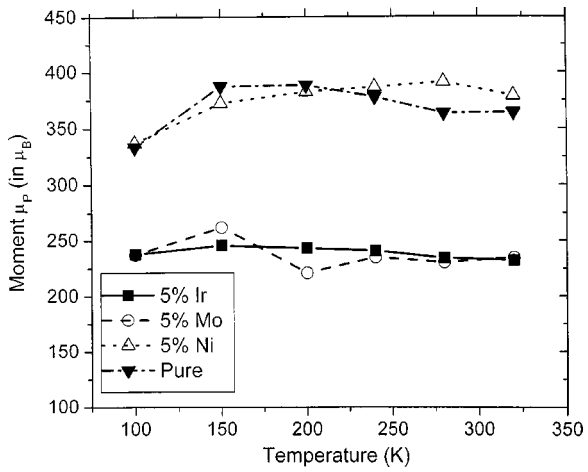

FIG. 8. The magnitudes of μ_p (magnetic moment/particle) estimated from the Langevin fits in Fig. 6 at different temperatures. The lines connecting the points are drawn for clarity.

C. Magnetization and hysteresis below T_p

The hysteresis loops were measured at 5 K under the ZFC and FC condition, by cooling the samples from 390 to 5 K in zero field and in $H=50$ kOe, respectively. The full loops to ± 50 kOe are shown in Fig. 9, whereas details of the loops for the lower H values are shown in Fig. 10. The magnitudes of the hysteresis loop parameters, viz., the coercivity H_c, remanence M_r, and loop shift H_e for the four samples, are listed in Table II. For the four samples of FHYD, Ni/FHYD, Mo/FHYD, and Ir/FHYD, H_c values are higher for the ZFC samples as compared to the FC samples. Conversely, the remanence M_r is increased for the FC cases. Thus the loops become narrower and taller for the samples cooled in 50 kOe. This is interesting since most antiferromagnetic nanoparticles below their blocking temperatures show a significant increase in the loop width accompanied with strong exchange bias when field-cooled from $T>T_N$.[4,6,9,10] The

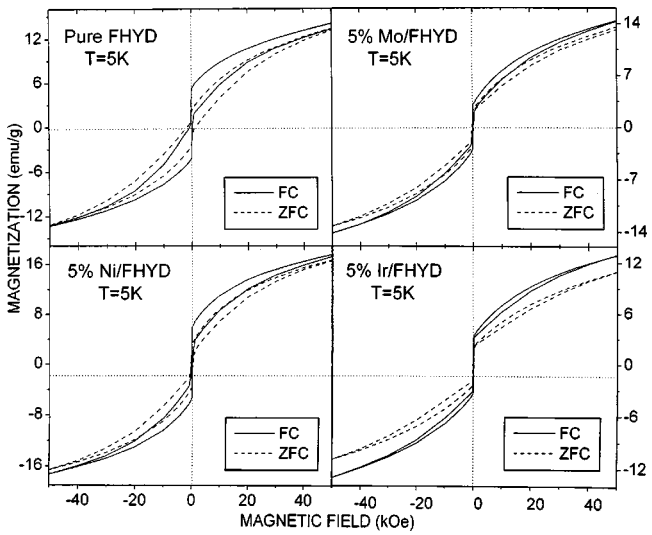

FIG. 9. Hysteresis loops of the four samples at 5 K measured up to ± 50 kOe. For the FC case, the samples were cooled from 390 to 5 K in 50 kOe.

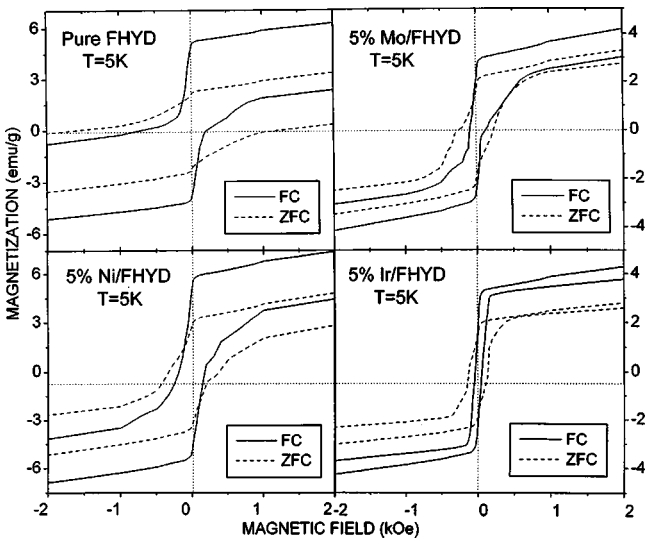

FIG. 10. The low-field portions (up to ± 2 kOe) of the hysteresis loops for the four samples at 5 K, showing coercivity and loop shift.

magnitudes of H_c decrease with doping in all cases in the order FHYD, Ni/FHYD, Mo/FHYD, and Ir/FHYD. The largest changes are for the Ir/FHYD sample, in which H_c is lowered by an order of magnitude whereas M_r is lowered by a factor of about 2. The areas of the loops for the FC and ZFC samples at 5 K are listed in Table II. The areas decrease in the order FHYD, Ni/FHYD, Mo/FHYD, and Ir/FHYD, the same order as for H_c noted above. A very interesting result observed here is the appearance of steps in the hysteresis loops in the low-field region for all the four samples (Fig. 10). It can be seen that the larger width (or coercivity) of the ZFC loop as compared to the FC loop is related to the differences in the slopes and plateaus of the steplike features. To illustrate the temperature dependence, steplike features observed in pure FHYD at different temperatures are shown in Fig. 11.

For the undoped FHYD, we carefully measured the hysteresis loop parameters both for the ZFC and FC (in 50 kOe from 390 K) cases as a function of temperature. The temperature variation of M_r is shown in Fig. 12(a) and that of H_c in Fig. 12(b). Above about 30 K, the magnitudes of H_c and M_r for the FC and ZFC cases agree, whereas below this temperature the magnitudes of H_c for FC are lowered and those of M_r are enhanced as compared to the ZFC case. From the data shown in Fig. 3 and Table I, $T_s=30$ K is the temperature at which a minimum in the FC susceptibility is observed. Thus the effects of FC *vis-à-vis* ZFC are particularly prominent at temperatures below T_s.

IV. DISCUSSION

For nanoparticles each with volume V and obeying superparamagnetism, the Neel-Arrhenius relation for the relaxation time τ for switching of the magnetization across the anisotropy barrier K_aV is usually written as

$$\tau=\tau_0 \exp(K_aV/kT), \tag{4}$$

TABLE II. Hysteresis loop parameters of FHYD, Ni/FHYD, Mo/FHYD, and Ir/FHYD.

	Field cooling to 5 K at 50 kOe from 390 K			Zero-field cooled to 5 K from 390 K			Loop shift
Material	H_c (Oe) (± 3)	M_r (emu/g) (± 0.1)	Loop area (a.u.) (± 0.5)	H_c (Oe) (± 5)	M_r (emu/g) (± 0.1)	Loop area (a.u.) (± 0.2)	H_E (Oe) (± 2)
Pure FHYD	470	5.1	16.7	1450	2.2	15.2	-250
5% Ni/FHYD	185	5.2	12.1	350	2.9	11.3	-7.5
5% Mo/FHYD	110	2.2	5.8	235	1.7	6.8	$+17$
5% Ir/FHYD	48	1.7	3.3	135	1.5	4.7	$+8$

where K_a is the anisotropy energy/volume and $\tau_0 \simeq 10^{-11}$ sec for FHYD.[16] The thermal switching of M gets blocked at a temperature T_B when τ becomes equal to τ_c, where τ_c is the characteristic time of measurements. Using $\tau_c \simeq 10^2$ sec for magnetometry yields

$$T_B \simeq K_a V/30k. \tag{5}$$

In a system with particle size distribution, T_B will have a distribution leading to the concept of an average $\overline{T_B}$. T_p the temperature at which ZFC peaks, is then given by $T_p = \beta \overline{T_B}$, with $\beta \simeq 1.5$–2.0 depending on the distribution function.[17,18]

From the data collected in Table I, the largest observed changes in FHYD on doping with Ni, Mo, and Ir occur in T_p, T_s, and μ_p. Since our samples have a particle size distribution (Figs. 1 and 2), T_p represents T_B for particles with the largest V. We note that the ratio T_p/T_s for the four samples varies between 1.75 and 2.3 (Table I) approximating β discussed above so that T_s appears to coincide with the expected $\overline{T_B}$. The data of Fig. 12 for undoped FHYD show that the coercivity H_c and remanence M_r go to zero at T_p. But below $T_s \simeq 30$ K, H_c is different for FC and ZFC cases and an exchange bias H_E appears for $T < T_s$. For undoped FHYD, our observations here for a minimum in χ (FC) at T_s and appearance of H_E for $T < T_s$ are similar to those reported for γ-Fe_2O_3 nanoparticles with $T_p \simeq 75$ K and $T_s \simeq 40$ K, in which $T_s \simeq 40$ K has been designated as a surface spin-glass transition.[19,20] Thus it is likely that in the FHYD, T_s represents a transition to a state with spin-glass-like ordering of the surface spins.

From Eq. (5), T_B varies linearly with K_a and V. For FHYD and Mo/FHYD, the particle size distributions are ac-

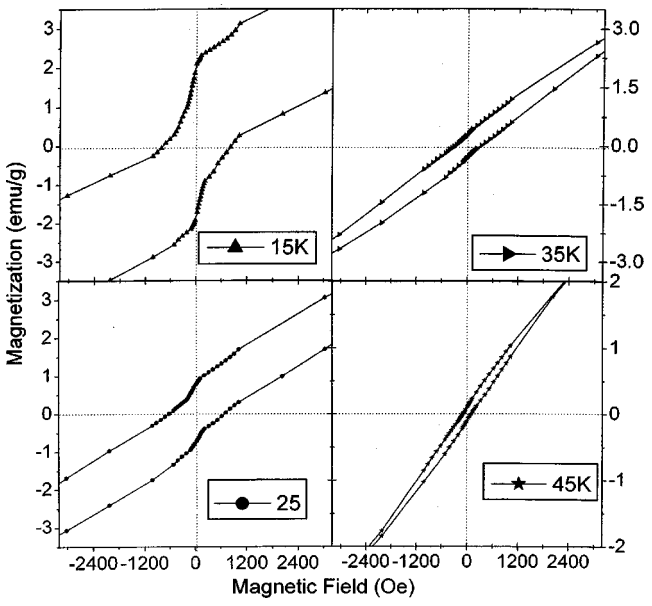

FIG. 11. The low-field regions of the hysteresis loops for the pure FHYD sample at 15, 25, 35, and 45 K measured after field cooling in 25 kOe from 390 K, showing the temperature variation of the steplike features.

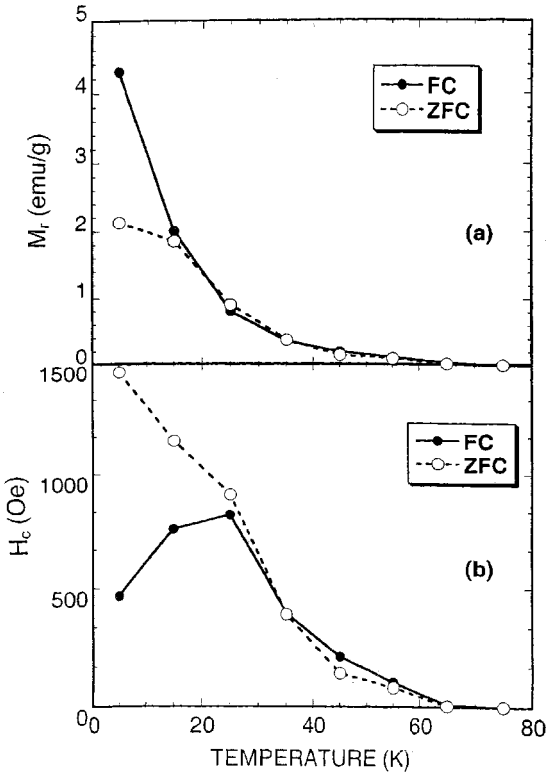

FIG. 12. Temperature variations of (a) M_r and (b) H_c for the undoped FHYD. For each data point, the sample was cooled from 390 K to the temperature of measurement in $H=0$ for ZFC and $H=50$ kOe for FC. The lines connecting the points are drawn for visual clarity.

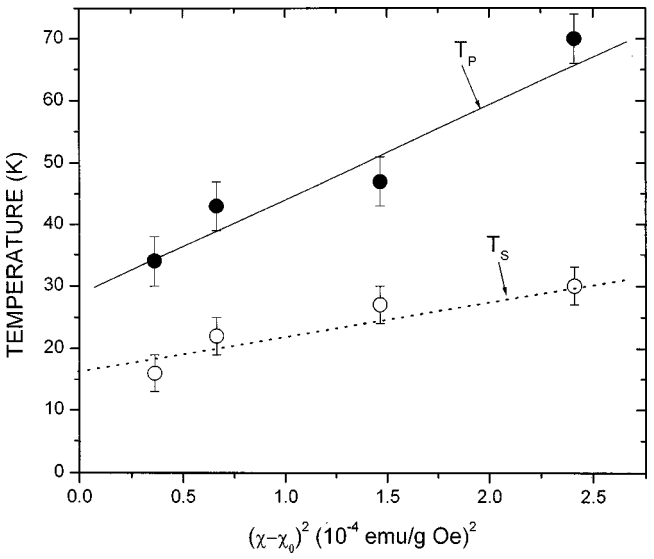

FIG. 13. Plots of T_p and T_s (Table I) as a function of $(\chi-\chi_0)^2$ at 330 K. The lines are linear ''eyeball'' fits.

curately known from TEM studies (Figs. 1 and 2) showing the distributions centered around 5 nm for FHYD and 5.5 nm for Mo/FHYD. Therefore, from size consideration alone, T_B for Mo/FHYD should be slightly higher than that for FHYD. Experimentally, T_B, T_s, and μ_p for Mo/FHYD are lower by 30–40 % than the corresponding values for FHYD (Table I). Therefore, according to the above analysis, anisotropy energy K_a for Mo/FHYD, as compared to that for FHYD, must be considerably lower. Although we were not able to accurately determine the particle size distributions for Ni/FHYD and Ir/FHYD due to the agglomeration problem mentioned earlier, the systematic decreases in T_p and T_s observed for these cases may also be due primarily to changes in K_a. The analysis presented below provides additional support for this argument.

The dominant contributions to K_a for NP systems come from magnetocrystalline anisotropy K_1 and shape anisotropy due to demagnetization energy K_d for nonspherical particles.[20] Since K_d varies as M^2, we have plotted T_p and T_s versus the magnitude of $(\chi-\chi_0)^2$ at 330 K (from Fig. 3) in Fig. 13. Reasonably linear variations are observed as expected from the above arguments with the intercept at $(\chi-\chi_0)^2=0$ presumably resulting from the magnetocrystalline anisotropy K_1. The above interpretation is consistent with the observed temperature variations of the EPR (electron paramagnetic resonance) linewidth ΔH and resonance field H_r in a number of systems including FHYD, where, as T approaches T_B from above, rapid increases in ΔH and decreases in H_r have been interpreted in terms of the shape anisotropy due to K_d.[20–22] Thus the observed changes in T_p and T_s may simply be related to decreases in μ_p (magnetic moment/particle) and the resulting lowering of the magnetic susceptibility χ. The observed decrease in the areas of loops upon doping (Table II) also indicates lowering of anisotropy since the loop area is proportional to magnetic anisotropy.[23]

The changes in μ_p on doping FHYD with Ni, Mo, and Ir noted above are another important result (Table I). Néel's model of nanoscale magnetism in antiferromagnetic materials predicted that the magnetic moment of the particles for $H\rightarrow 0$ depends on the uncompensated spins $p=n_A-n_B$, where n_A and n_B are the number of magnetic atoms on the two sublattices. For a particle of size d, the number n of atoms per particle with magnetic moment μ_p on each and interatomic distance of a is given by $n\sim d^3/a^3$. The dependence of p on n and hence d goes as follows: (i) $p=n^{1/2}$ for random distribution of missing B spins; (ii) $p=n^{2/3}$ if the top and bottom layers of a particle belong to the same sublattice; and (iii) $p=n^{1/3}$ if only the alternating planes belonging to the same sublattice of the top and bottom layers are uncompensated. In undoped FHYD, the observed $\mu_p\simeq 369\mu_B$ from this work means that the number of uncompensated Fe^{3+} spins $p\simeq 63$ assuming $5.9\mu_B/Fe^{3+}$ ion.[12] With an average particle size of 5 nm, as obtained from the HRTEM data, and a 3-Å interatomic distance between the Fe^{3+} ions,[24] $n\simeq 4630$, of which 1025 ($\simeq$22% of n) will be on the surface of the particle. Since the estimated magnitude of p is relatively closer to $n^{1/2}$ among the three predicted situations, one would assume a random distribution of uncompensated spins in the nanoparticles based on Neel's arguments. If there is uniform substitution of the dopants for Fe^{3+} ions, then p will only change by 5% leading to $\mu_p\simeq 297\mu_B$ for the Mo- and Ir-doped samples, assuming no moment for the dopants. This is clearly not valid for Mo/FHYD and Ir/FHYD, where μ_p is lowered by $\simeq$35%, although for Ni/FHYD, this may be a possibility. On the other hand, pure FHYD displays strong exchange anisotropy at low temperatures, which clearly presents the picture of a spin-glass-like ordered surface layer and a compensated AF ordered core. This will be possible only if the particle moment of $369\mu_B$ of the pure FHYD is completely due to the surface Fe^{3+} spins alone, which amounts to 5% of the total Fe^{3+} spins on the surface. Using Mo K-edge EXAFS (extended x-ray-absorption fine-structure) spectroscopy in Mo/FHYD, Zhao *et al.*[24] have shown that Mo species are primarily at the surface of FHYD surrounded by three to four oxygen atoms at distances of 1.73–1.76 Å, which are typical distances for tetrahedrally coordinated $(MoO_4)^{2-}$. As noted in the Introduction, the coordination of the surface Fe^{3+} sites is tetrahedral as opposed to the octahedral coordination of the Fe^{3+} sites in the interior of FHYD. If the argument that the particle moment results from surface Fe^{3+} spins is valid, then 5% Mo doping should destroy the spin-glass-like ordering of the surface layer of uncompensated spins. In this case, the result will be the disappearance of exchange anisotropy H_E and lowering of the FC remanence M_r and μ_p significantly. The valence state of Mo in $(MoO_4)^{2-}$ is Mo^{6+}, which is diamagnetic and hence carries no magnetic moment, leading to the observed large decrease in μ_p for Mo/FHYD. Although Mo ions will preferably substitute for surface Fe^{3+} sites, they will replace both compensated and uncompensated Fe^{3+} ions on the particle surface. Since exchange anisotropy completely disappeared and both M_r and μ_p reduced considerably by 5% Mo doping, it is safe to conclude that the observed particle moment in ferrihydrite nanoparticles results from uncompensated surface spins. For Ir/FHYD, a similar absence of ex-

change anisotropy and the large drops in μ_p and M_r suggest a situation similar to that for Mo/FHYD, although both Ir^{3+} and Ir^{4+} should have a magnetic moment. For Ni^{2+} and Ni^{3+}, the Hund's rule moments are less than that of Fe^{3+}. Although the exchange anisotropy is reduced considerably in Ni/FHYD also, μ_p and M_r remain undiminished. This indicates that Ni ions probably occupy vacant Fe^{3+} sites and may substitute for Fe throughout the particle. This is corroborated by the XRD patterns, which show some improvement in crystallinity for Ni/FHYD and some decrease in crystallinity for Mo/FHYD and Ir/FHYD, using widths of the lines as a criterion. The relatively sharper XRD peaks and the larger magnitude of μ_p for Ni/FHYD may be attributed to a bigger particle size, but the lower values of T_p and T_s go against this possibility. Thus from this analysis, it is concluded that doping occurs primarily at the surface for Mo/FHYD and Ir/FHYD, whereas for Ni/FHYD, experimental evidence suggests Ni substituting for Fe throughout the nanoparticle.

Next, we consider the steplike features observed in the low H regions of the hysteresis loops of Figs. 10 and 11. These features became less pronounced as the temperature was increased from 5 K towards T_s and were completely absent for $T>T_s$. Such steps in the hysteresis loops have been predicted by the recent theoretical studies of Fraerman and Sapozhnikov[25] for a one-dimensional nanoparticle system with long-range interaction energy proportional to r^{-p}. The nature of the steps is determined by the competing effects of coercivity, interparticle interactions, and thermal energy. Wider (narrower) steps are due to interactions of the nearer (distant) magnetic moments, and an increase in temperature tends to smooth out the steps. Experimentally, Grundler *et al.*[26] have reported some steplike features in the hysteresis loops for arrays of single-domain Ni nanomagnets (13 nanomagnets with 600-nm spacings). The steps in the hysteresis loops observed in the FHYD samples (Figs. 10 and 11) in the low-field region could be due to the dipolar interparticle interactions since these particles are severely agglomerated. The spin-glass-like ordering of the surface spins may also be important to introduce the dipolar interparticle interactions so that the steps are observed only for $T<T_s$. More detailed investigation of these steplike features are currently underway. A more quantitative check on the theory by Fraerman *et al.*[25] requires a systematic variation of the interparticle separation r and measuring the effects of this variation on the hysteresis loops. Another feature of these results in samples cooled in a high magnetic field of 50 kOe from temperatures $T>T_p$ is that there is an increase in M_r and a decrease in H_c (Fig. 10). For FC samples, the surface moments are expected to align along the cooling field direction so that the changes in M_r and H_c are understandable.

V. SUMMARY AND CONCLUSIONS

Analysis of the M versus T and M versus H data at different T has been carried out in FHYD nanoparticles and FHYD doped with 5% each of Ni, Mo, and Ir. From the changes in the magnetic parameters observed upon doping, it is inferred that the particle moment in FHYD is due to uncompensated spins on the surface of the particles and that Mo and Ir preferentially substitute for the surface Fe^{3+} ions, and Ni appears to substitute for Fe throughout the nanoparticle. The ZFC susceptibility peaks at a temperature T_p, which is nearly twice the temperature T_s at which spin-glass ordering of the surface spins is indicated. The shift of T_p and T_s with doping suggests that a significant source of magnetic anisotropy in these particles is the shape anisotropy resulting from the demagnetizing fields. The steplike features observed in the low-field regions of the hysteresis loops might be due to the dipole-dipole interparticle interactions.

ACKNOWLEDGMENTS

This research was supported by the NSF-Idaho-EPSCoR Program and the National Science Foundation at Boise State University and by the U.S. Department of Energy Contract No. DE-FC26-99FT40540 and No. DE-FC 26-02NT41594 at West Virginia University and the University of Kentucky.

*Corresponding author. Email address: Mohindar.Seehra@mail.wvu.edu

[1] See the review by J. L. Jambor and J. E. Dutrizac, Chem. Rev. (Washington, D.C.) **98**, 2549 (1998), and references therein.

[2] J. Zhao, F. E. Huggins, Z. Feng, and G. P. Huffman, Phys. Rev. B **54**, 3403 (1996).

[3] M. M. Ibrahim, G. Edwards, M. S. Seehra, B. Ganguly, and G. P. Huffman, J. Appl. Phys. **75**, 5873 (1994).

[4] S. A. Makhlouf, F. T. Parker, and A. E. Berkowitz, Phys. Rev. B **55**, R14 717 (1997).

[5] J. Zhao, F. E. Huggins, Z. Feng, F. Lu, N. Shah, and G. P. Huffman, J. Catal. **143**, 499 (1993); J. Zhao *et al.*, *ibid.* **143**, 510 (1993); Clays Clay Miner. **42**, 737 (1994).

[6] See, e.g., R. H. Kodama and A. E. Berkowitz, Phys. Rev. B **59**, 6321 (1999).

[7] L. Néel, in *Low Temperature Physics*, edited by C. Dewitt, B. Dreyfus, and P. G. de Gennes (Gordon and Breach, New York, 1962), p. 413.

[8] J. T. Richardson, D. L. Yiagas, B. Turk, K. Forster, and M. V. Twigg, J. Appl. Phys. **70**, 6977 (1991).

[9] S. A. Makhlouf, F. T. Parker, F. E. Spada, and A. E. Berkowitz, J. Appl. Phys. **81**, 5561 (1997).

[10] A. Punnoose, H. Magnone, M. S. Seehra, and J. Bonevich, Phys. Rev. B **64**, 174420 (2001).

[11] M. S. Seehra and A. Punnoose, Phys. Rev. B **64**, 132410 (2001).

[12] M. S. Seehra, V. S. Babu, A. Manivannan, and J. W. Lynn, Phys. Rev. B **61**, 3513 (2000).

[13] J. Zhao, Z. Feng, F. E. Huggins, and G. P. Huffman, Energy Fuels **8**, 38 (1994).

[14] M. S. Seehra, V. S. Babu, P. Roy, and A. Manivannan, in *Cluster and Nanostructure Interfaces*, edited by P. Jena, S. N. Khanna, and B. K. Rao (World Scientific, Singapore, 2000), pp. 229–234.

[15] The magnitude of χ/g at $T=T_p$ for FHYD in Fig. 3 is different from that reported earlier for deuterated FHYD (Ref. 12) and dehydrated FHYD (Ref. 3) and FHYD (Ref. 11). These differ-

ences can be understood in terms of the different densities of these materials because of the different degrees of hydration, leading to different concentrations of Fe^{3+} ions/g of the material. Although T_p is nearly identical, χ/g (in units of 10^{-4} emu/g Oe) of pure FHYD at T_p equals 10 in this work, 6.5 for deuterated FHYD with higher density (Ref. 12) and 30 for dehydrated FHYD, with much lower density (Ref. 3). Aging of a FHYD sample at room temperature affects density due to hydration and hence the measured χ/gm (Ref. 11).

[16] M. M. Ibrahim, S. Darwish, and M. S. Seehra, Phys. Rev. B **51**, 2955 (1995).

[17] J. I. Gittleman, B. Abeles, and S. Bozoeski, Phys. Rev. B **9**, 3891 (1974).

[18] M. El-Hilo, K. O'Grady, and R. W. Chantrell, J. Magn. Magn. Mater. **114**, 295 (1992); **117**, 21 (1992).

[19] B. Martinez, X. Obradors, L. Balcells, A. Rouanet, and C. Monty, Phys. Rev. Lett. **80**, 181 (1998).

[20] Yu. A. Koksharov, S. P. Gubin, I. D. Kosobudsky, G. Yu. Yurkov, D. A. Pankratov, L. A. Ponomarenko, M. G. Mikheev, M. Beltran, Y. Khodorkovsky, and A. M. Tishin, Phys. Rev. B **63**, 012407 (2000).

[21] R. Berger, J.-C. Bissey, J. Kliava, H. Daubric, and C. Estournes, J. Magn. Magn. Mater. **234**, 535 (2001).

[22] M. S. Seehra, A. Punnoose, P. Roy, and A. Manivannan, IEEE Trans. Magn. **37**, 2207 (2001).

[23] E. C. Stoner and E. P. Wohlfarth, Philos. Trans. R. Soc. London, Ser. A **240**, 599 (1948).

[24] J. Zhao, Z. Feng, F. E. Huggins, N. Shah, G. P. Huffman, and I. Wender, J. Catal. **148**, 194 (1994).

[25] A. A. Fraerman and M. V. Sapozhnikov, Phys. Rev. B **65**, 184433 (2002).

[26] D. Grundler, G. Meier, K. B. Broocks, Ch. Heyn, and D. Heitmann, J. Appl. Phys. **85**, 6175 (1999).